Published in final edited form as:

Obesity (Silver Spring). 2022 November ; 30(11): 2122–2133. doi:10.1002/oby.23538.

Monoacylglycerol O-acyltransferase 1 lowers adipocyte differentiation capacity *in vitro* but does not affect adiposity in mice

Jason M. Singer[1], **Trevor M. Shew**[1], **Daniel Ferguson**[1], **M. Katie Renkemeyer**[1], **Terri A. Pietka**[1], **Angela M. Hall**[1], **Brian N. Finck**[1], **Andrew J. Lutkewitte**[1,*]

[1]Center for Human Nutrition, Washington University School of Medicine, St. Louis, MO

Abstract

Objective: Monoacylglycerol O-acyltransferase 1 (*Mogat1*), a lipogenic enzyme that converts monoacylglycerol to diacylglycerol, is highly expressed in adipocytes and may regulate lipolysis by re-esterifying fatty acids released during times when lipolytic rates are low. However, the role of *Mogat1* in regulating adipocyte fat storage during differentiation and diet-induced obesity is relatively understudied.

Methods: Here we generated adipocyte-specific *Mogat1* knockout mice and subjected them to a high-fat diet to determine the effects of *Mogat1* deficiency on diet-induced obesity. We also used *Mogat1* floxed mice to develop preadipocyte cell lines wherein *Mogat1* could be conditionally knocked out to study adipocyte differentiation *in vitro*.

Results: In preadipocytes, we found that *Mogat1* knockout at the onset of preadipocyte differentiation prevented the accumulation of glycerolipids and reduced the differentiation capacity of preadipocytes. However, the loss of adipocyte *Mogat1* did not affect weight gain or fat mass induced by a high-fat diet in mice. Furthermore, loss of *Mogat1* in adipocytes did not affect plasma lipid or glucose concentrations or insulin tolerance.

Conclusions: These data suggest *Mogat1* may play a role in adipocyte differentiation *in vitro* but not adipose tissue expansion in response to nutrient overload in mice.

Keywords

adipogenesis; monoacylglycerol; obesity; lipids

INTRODUCTION

Adipose tissue regulates systemic metabolism through endocrine factors (adipokines) and the regulated storage and release of free fatty acids (FFA) and glycerol. Triglycerides (TAG) comprise three fatty acids esterified to a glycerol backbone and represent the most abundant lipid species stored within adipocytes. In higher organisms, two pathways have evolved

*Acceptance of proofs and correspondence to Andrew J. Lutkewitte: alutkew@wustl.edu, Center for Human Nutrition, Washington University School of Medicine, 660 Euclid Ave., Box 8031, St. Louis, MO 63110, United States.

Disclosures: The authors have no disclosures.

for TAG synthesis converging at diacylglycerol (DAG); the glycerol-3-phosphate and the monoacylglycerol O-acyltransferase (MGAT) pathways. The MGAT family of enzymes acylate monoacylglycerol (MAG) into DAG, most of which is directly acylated into TAG via diacylglycerol O-acyltransferase (DGAT) activity. In humans, three genes encode enzymes of this family (*MOGAT1*, *MOGAT2*, and *MOGAT3*), but there are only two *Mogat* family genes (*Mogat1* and *Mogat2*) in mice. *Mogat2* is enriched in intestinal enterocytes and is important for dietary fat absorption (1–3). In contrast, *Mogat1* is highly induced in liver of mice with hepatic steatosis and is the primary MGAT isoform expressed in adipose tissue of humans and rodents (4–6). While intestinal MGAT function has been studied for many years, less is known about the physiologic function of MGAT in other organs. We have recently shown that hepatic *Mogat1* deletion does not affect hepatic steatosis and insulin resistance, while germline deletion actually exacerbates these conditions during diet-induced obesity (7). However, it remains to be determined whether modulating MGAT activity in adipose tissue specifically might have efficacy for preventing or treating obesity-related metabolic disease.

Mogat1 expression and MGAT activity are highly induced during the differentiation of mouse and human precursors cells into mature adipocytes (4). Adipose tissue *Mogat1* gene expression is reduced in genetic models of marked obesity (*db/db* mice) and abdominal fat of people with obesity that exhibit metabolic abnormalities compared to people with metabolically-healthy obesity (4). Indeed, adipose tissue *MOGAT1* positively correlates to glucose disposal rates during hyperinsulinemic-euglycemic clamps in people with obesity (4). However, the cause and effect relationship between these observations requires further study.

Several questions remain regarding the role of *Mogat1* in adipocyte differentiation and function. For example, although *Mogat1* expression is highly induced early in the adipogenic program (4), the requirement for *Mogat1* in adipocyte differentiation remains unclear. Does diminished adipose tissue MGAT activity lead to ectopic fat accumulation and metabolic abnormalities with nutrient overload? Few studies have addressed the requirement for *Mogat1* in adipose tissue expansion during the progression of obesity (8–10) and those that have, used global knockout of *Mogat1* rather than deleting in an adipocyte-specific manner. We have recently shown global deletion of *Mogat1* leads to unexpected increases in weight gain in mice fed a high-fat diet (7). Herein, we sought to determine the functional consequences of *Mogat1* depletion during adipocyte differentiation *in vitro* and expansion *in vivo* by using mice harboring a floxed allele of *Mogat1* and by generating adipocytes with conditional deletion of *Mogat1*.

METHODS

Animal studies.

All mouse studies were approved by the Institutional Animal Care and Use Committee of Washington University. *Mogat1* whole body null mice and adipocyte-specific *Mogat1* knockout mice were generated as previously described (4, 7 and described in supplemental methods). All mice were backcrossed onto the C57BL/6J background. Littermate controls

were all homozygous for the *Mogat1* floxed allele. Mice were group-housed and given free access to food and water and subjected to a 12 h light/dark cycle.

Eight-week-old male and female mice were given either a control low-fat diet (LFD, Research Diets, 10 kcal % fat, D12450J) or a high-fat diet (HFD, Research Diets, 60 kcal % fat, D12492) for the duration indicated. Before sacrifice, mice were fasted for 4 h starting at 0900 and were euthanized via CO_2 asphyxiation. Blood was collected from venipuncture of the inferior vena cava into EDTA-coated tubes and plasma was removed by centrifugation. Adipose and other tissues were collected, flash-frozen in liquid nitrogen, and stored at −80°C until further use.

Metabolic phenotyping.

Glucose tolerance tests (GTT) were performed in 5 h fasted mice with the fasting beginning at 0900. Glucose was dissolved in saline and mice were given intraperitoneal (IP) injections (1 g glucose/kg lean mass). Insulin tolerance tests (ITT) were performed on mice fasting for 4 h starting at 0900. Insulin was given as an IP injection of recombinant Humulin R® (0.75 U/kg lean mass in saline). Blood glucose was measured from tail blood using a One Touch Ultra glucometer (Life Scan Inc.). Lean and fat mass were determined in fed mice by ECHO MRI.

Adipocyte sizing and counting.

Adipocyte size and number were measured as previously described (11, 12). Briefly, harvested inguinal and gonadal white adipose tissue (iWAT and gWAT, respectively (25–50 mg)) was fixed in 0.2 mol/L collidine HCl/31 mg/mL osmium tetraoxide solution for 30 days followed by dissociation with 8 mol/L urea and 154 mmol/L NaCl. Liberated adipocytes were measured using a 400-micrometer aperture on a Multisizer 3 (Beckman Coulter).

Plasma analytes.

Plasma lipids were determined using commercially available kits: triglycerides (Infinity Triglyceride colorimetric assay kit (Thermo Fisher, TR22421)), NEFA (WAKO), and free glycerol reagent (Sigma, F6428).

Isolation of stromal vascular fractions (SVF).

Male or female mice were euthanized via CO_2 asphyxiation and iWAT was isolated under sterile conditions (13). The resulting fat pads were rinsed in PBS and minced in ice-cold digestion buffer (7.5 mg/ml Collagenase D (Roche 1108886001), and 4.8 mg/ml Dispase II (Sigma D4693) in PBS with 10 mM calcium). Samples were incubated in digestion buffer for 5 min in a 37°C water bath and transferred to an orbital shaker at 37°C / 5% CO_2 for 30–40 min. Following incubation, cells were passed through a 70-micron filter and centrifuged at 700 x g for 5 min. The resulting SVF cells were washed in PBS before red blood cell lysis (ACK lysing buffer, Gibco A10492). The cell pellet was washed twice more with PBS before plating (DMEM F-12, 10% FBS, 100 U/mL PenStrep) and allowed to expand before differentiation or immortalization.

Immortalization and generating of conditional knockout cells

SVF cells were isolated as above and on the same day a confluent 10 cm dish of 293T cells was transfected with 1.5 μg psPAX2 lentiviral packaging vector (Addgene 12260), 1.5 μg pMD2.G envelop plasmid (Addgene, 12259), and 3 μg pBABE-neo largeT antigen cDNA (Addgene, 1780 ref (14))using lipofectamine 2000 (Invitrogen, 11668019). Three days after the SVF media was replaced with media from the transfected 293T cells that was filtered and mixed at a 1:1 ratio with standard SVF media and viral media with added polybrene (8 μg/mL, Millipore Sigma TR-10030). The infected cells were selected for using Geneticin (G418 Sulfate, 0.2 mg/mL). Conditional knockout cells were generated by infection with media from a confluent 10 cm dish of 293T cells transfected with 3 μg pCL-Eco (Addgene, 12371 ref (15)) and 3 μg MSCV CreERT2 puro (Addgene, 2276 ref (16)) and polybrene (8 μg/mL, Millipore Sigma TR-10030). Cells were selected by puromycin (2 μg/mL) and maintained in DMEM F-12 (10% FBS).

Differentiation of adipocytes.

All cells were allowed to become confluent. The following day (day 0) cells were treated with a differentiation cocktail mix (DIXγ: 1 μM dexamethasone, 2 μg/mL insulin, 500 μM 3-isobutyl-1–1methylxathine (IBMX), and 15 μM troglitazone). Every 2 days thereafter, the media was replaced with maintenance media (DMEM with 2 μg/mL insulin) for days indicated (5, 6, or 10 days). For knockdown studies, Cre-ERT2 recombinase was activated via 4 nM tamoxifen (TAM) on days indicated (13). All experiments were performed in triplicate and replicated in at least three independent experiments.

Oil Red O staining and quantification.

Oil Red O staining was performed in 12 well plates on days indicated. Cells were rinsed in PBS and fixed with 10% formalin for 60 min at room temperature. Fixed cells were washed in deionized water and dehydrated with 60% isopropanol for 5 min. Oil Red O was prepared according to the manufacturer's suggestions (Sigma O0625). Neutral lipids were stained for 5 min at room temperature, and excess Oil Red O was removed and rinsed in deionized water until clear. Oil Red O was extracted by 100% isopropanol for 5 min and absorbance was read at 492 nm.

mRNA isolation, quantification, and Bulk RNA sequencing.

Total RNA was isolated from cells or frozen adipose tissue samples using Trizol™ Plus RNA Purification System (Thermo Fischer, 12183555) according to the manufacturer's protocol. 2 μg RNA was reverse transcribed into cDNA using Taqman high-capacity reverse transcriptase (Life Technologies, 43038228). Quantitative PCR was performed using Power SYBR green (Applied Biosystems, 4367659) and measured on an ABI PRISM 7500 or ABI QuantStudio 3 sequence detection system (Applied Biosystems). Results were quantified using the $2^{-\Delta\Delta Ct}$ method and shown as arbitrary units relative to control groups. Primer sequences are listed in Table S1. Bulk RNA sequencing and analysis were performed at the Genome Technology Access Center at the McDonnell Genome Institute of Washington University School of Medicine. A detailed description is available in the supplemental materials.

Lipidomic analysis.

Lipidomic analysis was performed at the Washington University Metabolomics Facility. Immortalized SVF cells (5×10^6) were grown in 10 cm dishes and treated with vehicle or DIXγ for 10 days. Following differentiation, cells were pelleted in 500 μl PBS, frozen in liquid nitrogen, and stored at −80°C until analysis. Lipids were extracted in the presence of their internal standards. MAG, DAG, and TAG species were extracted using the Bligh and Dryer method (17) and PA was extracted using protein precipitation before LC-MS/MS analysis. Peak area ratios of each analyte were determined from the internal standards. Quality control (QC) samples were prepared by pooling an aliquot of each study sample and ejected every four study samples. Only species with CV %, 15% for the QC injections were reported. Data are reported as fold change from undifferentiated vehicle-treated cells.

Statistical analysis.

Data were analyzed using GraphPad Prism software. One-way analysis of variance (ANOVA) or factorial ANOVAs were performed where appropriate. Secondary post-hoc analysis found differences in groups using either Tukey's or Dunnett's multiple comparisons were appropriate. $p < 0.05$ was considered significant.

RESULTS

Mogat1 is required for adipocyte differentiation *in vitro*.

Mogat1 expression and activity are highly induced during the differentiation of mouse and human adipocytes *in vitro* (4), but whether this is critical to the differentiation process is unclear. To this end, we isolated SVF cells from iWAT and differentiated them using a standard differentiation cocktail (DIXγ: 1 μM dexamethasone, 2 μg/mL insulin, 500 μM IBMX, 15 μM troglitazone) (Figure S1A and refs 4, 15). SVFs from wild-type mice had typical increases in adipogenic gene expression reaching maximal expression around day six-post DIXγ treatment (Figure S1B). *Mogat1* expression was induced nearly 100-fold in differentiated compared to undifferentiated cells, while *Mogat2* expression decreased during differentiation (Figure S1C and ref (18)). However, we found that SVF cells from germline *Mogat1* null mice differentiated normally (Figure S2), which is consistent with our previous studies indicating germline deletion of *Mogat1* does not alter adiposity in mice (7).

To avoid potential compensation of other enzymes with MGAT activity, which are induced during differentiation (Figure S1C), we utilized SVF cells isolated from *Mogat1* floxed mice to generate stable cell lines with an inducible Cre-ERT2 recombinase system (13). Following isolation, the cells were immortalized using SV40 T-antigen and then transfected with an inducible Cre-ERT2 (Figure 1A). After reaching confluency (day −1), the following day (day 0), cells were treated with TAM (or vehicle) and medium containing DIXγ (Figure 1A). Vehicle-treated cells differentiated as expected as indicated by increased Oil Red O staining of neutral lipids (Figure 1B). However, *Mogat1* knockout cells had decreased Oil Red O accumulation (Figure 1B). Importantly, TAM exposure alone is not sufficient to suppress differentiation in *Mogat1* floxed or wild-type SVF cells (Figure S3). *Mogat1* was highly induced by differentiation in control cells, but TAM treatment reduced differentiation-induced *Mogat1* gene expression without affecting *Mogat2* (Figure 1C).

Given the diminished capacity to accumulate lipids with *Mogat1* knockout, we also analyzed the expression of several key regulators of adipocyte differentiation (Figure 2). Expression of *Adipoq*, *Pparg1*, *Pparg2*, *Srebf1*, and *Fasn* were highly induced during differentiation in control cells (Figure 2A–E). However, the activation of these genes was markedly blunted in *Mogat1* knockout cells (Figure 2A–E). These data suggest *Mogat1* expression is indispensable for the initiation of adipocyte differentiation of SVF-derived preadipocytes *in vitro*.

Mogat1 deletion prevents glycerolipid accumulation in differentiated adipocytes.

Next, we performed lipidomic analyses to determine the effects of differentiation and *Mogat1* knockout on glycerolipid intermediate abundance (Figure 3A). We found several MAG species were decreased following differentiation and this was unaffected by *Mogat1* knockout (Figure 3B). Interestingly, in wild-type cells that were differentiated, the abundance of MAG(20:4) and MAG(22:6) were extremely low compared to undifferentiated cells (Figure 3B). However, these MAG species were significantly higher in *Mogat1* knockout adipocytes compared to wild-type adipocytes. The product of MGAT activity, DAGs, were increased in differentiated cells compared to undifferentiated cells and many highly abundant DAGs were reduced by *Mogat1* knockout including saturated and monounsaturated DAG(16:0/X) and DAG(16:1/X) species (Figure 3C). Several long-chain highly unsaturated DAGs were decreased during differentiation independent of *Mogat1* expression (Figure S4A, B). TAG species followed a similar trend as DAGs (Figure 3D and Figure S4–C). The DAG precursor and lipin enzymatic substrate, phosphatidic acids (PA), were mostly decreased by differentiation (Figure 3E), but PA(34:1) and PA(34:2) remained stable in controls cells and were reduced by *Mogat1* knockout.

Finally, we analyzed the expression of genes that encode glycerolipid metabolic enzymes in these cells (Figure 4A). The expression of the lipolytic genes *monoacylglycerol lipase* (*Mgll*), *hormone-sensitive lipase* (*Hsl*), and *adipose triglyceride lipase* (*Atgl*) were increased during differentiation and attenuated by *Mogat1* knockout (Figure 4B). Similarly, the expression of the glycerol-3-phosphate (G-3-P) pathway genes *glycerol-3-phosphate acyltransferase 2* (*Gpat2*) and *1-acylglycerol-3-phosphate O-acyltransferase* (*Agpat2*) *was also attenuated, while Gpat4* and *Agpat1* were increased by *Mogat1* knockout in undifferentiated cells (Figure 4C). Interestingly, in these cells, expression of *Lpin2,* but not *Lpin1* increased during differentiation and was not affected by the loss of *Mogat1*. *Lpin3* expression was increased by *Mogat1* knockout in differentiated cells (Figure 4D). The final step in both the MGAT and G-3-P pathways of TAG synthesis requires *Dgat1* or *Dgat2* and both genes were induced during differentiation, but attenuated by *Mogat1* knockout (Figure 4E). These data suggest that *Mogat1* is required for preadipocytes to fully differentiate and store glycerolipids *in vitro* and demonstrate isoform-specific effects of both differentiation and *Mogat1* knockout on the expression of enzymes in the G-3-P pathway.

Adipocyte-specific *Mogat1* knockout mice gain similar fat mass as littermate controls on a high-fat diet.

We have previously reported that, compared to wild-type littermate controls, mice with adipocyte-specific *Mogat1* knockout (Adn-*Mogat1*−/− mice) have reduced fat mass on a

chow diet, while whole-body *Mogat1* null mice have increased body weight on HFD (4, 7). To further evaluate the functional role of *Mogat1* in adipose tissue expansion we challenged male and female Adn-*Mogat1*−/− mice and their floxed littermate controls with a HFD (60% kcal from fat) or matched LFD (10% kcal from fat, matched sucrose) for 16 weeks (Figure 5 and Figure S5). Male Adn-*Mogat1*−/− mice fed HFD gained similar body weight and fat mass on the HFD compared to littermate controls on HFD (Figure 5A, B). Individual fat pad mass was also unaffected by genotype (Figure 5C–E). Similar results were found in high-fat-fed female mice (Figure S5A–C). WAT samples were fixed and dissociated and subsequently liberated adipocyte sizes were measured by a particle counter. The volume and diameter of individual iWAT adipocytes were increased by the HFD in wild-type mice but not in the Adn-*Mogat1*−/− mice and there were no differences between genotypes (Figure 5F). There were also no differences in cell volume, diameter, or number per mg tissue of gWAT between groups (Figure 5G). These data indicate adipocyte *Mogat1* expression does not affect the adiposity or adipocyte size and number in mice fed a HFD.

Adipocyte-specific *Mogat1* knockout does not improve glucose or insulin tolerance.

We have previously shown that *Mogat1* regulates basal lipolysis in adipose explants and 3T3-L1 cells suggesting that loss of *Mogat1* in adipocytes could lead to increased plasma lipids (4). However, plasma TAG, FFA, and glycerol were not different between genotypes on either diet (Figure 6A–C).

We performed glucose and insulin tolerance tests in adipocyte-specific *Mogat1* knockout mice and littermate controls. HFD feeding lead to glucose and insulin intolerance, but there was no difference in tolerance between genotypes on either diet (Figure 6D, E). Likewise, plasma insulin concentrations were increased by HFD, but similar between groups (Figure 6F). Analogous results were observed in female mice fed a HFD (Figure S5D, E). Liver weight did not change but HFD increased hepatic TAG content in both genotypes (Figure 6G, H). These data indicate adipocyte-specific *Mogat1* knockout mice have similar adiposity in response to a HFD as the littermate controls and adipocyte *Mogat1* expression does not affect systemic lipid or glucose metabolism.

Transcriptomic analysis of iWAT tissue from adipocyte-specific *Mogat1* knockout mice reveals few differences between genotypes.

We first assessed the expression of several lipogenic enzymes using RNA from iWAT from mice on either low fat or HFD. We did not detect any significant increase in the expression of DAG or TAG synthesizing genes (*Mogat2, Dgat1, Dgat2,* and *Lpin1*) (Figure 7A and Figure S8) that might compensate for the lack of *Mogat1* between genotypes (Figure 7B and refs (1, 6, 7, 19, 20). However, *Mogat2* was increased nearly forty-fold by high-fat diet in both genotypes. Expression of classic markers of adipocyte lipogenesis were also unaffected by *Mogat1* deletion except for fatty acid synthase (*Fasn*) which was increased in LFD-fed *Mogat1* knockout mice compared to littermate controls. (Figure 7C).

To better understand the molecular pathways affected by adipocyte-specific *Mogat1* deletion, we performed bulk RNA sequencing on iWAT from Adn-*Mogat1*−/− mice and their littermate controls after 16 weeks on HFD. This analysis revealed very few differences

between genotypes (Figure S6). In fact, only *Mogat1* was significantly decreased and 5 genes significantly increased given our criteria (adjusted p-value < 0.05, $\log_2$ FC < 2.0, Figure S6B, C). Pathway analysis identified several significantly downregulated GO biological process pathways including those related to fatty acid metabolism and oxidation (Figure S7A, B). KEGG pathways analysis showed there are alterations in metabolic pathways including insulin signaling, TCA cycle, and oxidative phosphorylation (Figure S7C, D). However, these pathways do not translate to any physiological measurements seen in these mice (Figures 5, S5, and 6).

DISCUSSION

Esterification and storage of FFA as neutral TAG in adipocytes is vital for preserving systemic metabolic health. Multiple enzymatic pathways have evolved to synthesize TAG including the MGAT pathway (Figure 4A). MGAT activity and function have been extensively characterized in intestine (2, 19, 21, 22) and liver (5, 7, 9, 10, 20, 23–25). However, few studies have evaluated MGAT function in adipocytes. We have previously shown adipocyte *Mogat1* ablation lowers fat mass by about 10%; however, these studies were conducted in young chow-fed mice (4). Here we demonstrate that *Mogat1* is dispensable for adipose tissue expansion in chronic high-fat-fed mice. We confirmed our previous report that *Mogat1* is the predominant MGAT isoform enriched during *in vitro* differentiation of mouse preadipocytes (Figure S1 and ref. (4)). Although, germline *Mogat1* null preadipocytes differentiated as expected (Figure S2), acute knockout of *Mogat1* using the preadipocytes with the conditional *Mogat1* allele severely blunted differentiation (Figures 1–4). *Mogat1* conditional knockout cells had reduced neutral lipid accumulation and expression of pro-adipogenic genes like *Pparg1, Pparg2, Srebf1,* and *Fasn*. Lastly, acute *Mogat1* ablation prevented lipid accumulation including most abundant DAG and TAG species during differentiated mouse adipocytes. The timing of *Mogat1* ablation and its effects on differentiation may warrant further investigation in future studies.

We previously demonstrated that *Mogat1* is dispensable for hepatic MGAT activity and steatosis development in obese mice suggesting compensation by alternative enzymes with MGAT activity and/or alternative sources for cellular TAG (7). In the present study, the loss of *Mogat1* in adipocytes does not alter adiposity (i.e. TAG accumulation) in diet-induced obese mice. This is not surprising given the functional redundancy of the lipid synthetic pathways. Lessons from *in vitro* studies imply that the acyltransferases, DGAT1 and DGAT2, are functionally redundant and compensate for the loss of either isoform in genetic deletion studies. The knockout of both DGAT isoforms is required to inhibit *in vitro* adipocyte differentiation (26). In adipose tissue specifically, DGAT1 completely compensates in adipose-specific DGAT2 knockout mice, while DGAT1 knockout mice are modestly leaner than their wild-type counterparts (27, 28). Furthermore, in the present study, we found that the adipose tissue expression of *Mogat2*, which is normally very low, is markedly increased by HFD feeding in mice (Figure 7B). This is important given that MGAT2 has a higher specific activity than MGAT1 (1). It is possible that the activity of MGAT2 and other enzymes capable of mediating TAG synthesis overcomes any effect of *Mogat1* deficiency.

Constitutive *Mogat1* deletion does not alter adipocyte differentiation both *in vivo* and *in vitro*, yet acute loss at the onset of differentiation *in vitro* almost completely prevents glycerolipid accumulation and activation of the differentiation program. In addition, the adiponectin-Cre-driven deletion, which occurs after differentiation has commenced, does not affect differentiation *in vivo*. This could suggest that *Mogat1* plays a critical role at a very specific early time in the differentiation program and that chronic loss of *Mogat1* results in compensatory effects. Although we have not identified a specific enzyme with compensatory activity, lipin family proteins also generate DAG. Although MGATs and lipins converge on DAG synthesis (the penultimate step in TAG synthesis) the physiological consequences of inhibiting these pathways are dissimilar *in vitro* and *in vivo* (2–4, 29–31). In contrast to prior work in other adipogenic cells (18, 32–34), *Lpin1* and *Lpin3* expression are modestly increased during our differentiation of the SVF-derived cell lines (Figure 4D). Genetic loss of *Lpin1* leads to dramatic impairments in adipogenesis both *in vitro* and *in vivo* (35, 31, 33, 32). This suggests the possibility that the failure of this particular *in vitro* model to increase *Lpin1* expression during differentiation might explain the dramatic reliance on *Mogat1* in this context and the differences with the *in vivo* phenotype.

Our lipidomics analysis revealed that the most abundant DAG and TAG species accumulate with differentiation and are reduced by *Mogat1* knockout (Figure 3 and Figure S3). In contrast, many MAG and PA species were reduced during differentiation suggesting that these precursors are consumed to drive DAG and TAG synthesis. Lipidomic analysis has increased the breadth of knowledge regarding the importance of specific fatty acyl chains of glycerol/phospholipids in metabolic regulation. Specific to this study, both arachidonic acid (20:4) and docosahexaenoic acid (22:6) have been shown to inhibit preadipocyte differentiation *in vitro* (36–38). In the present studies, MAG(20:4) and MAG(22:6) were abundant in undifferentiated cells, but not in differentiated wild-type adipocytes. The reduction that occurred during differentiation was attenuated by *Mogat1* ablation. Yen and colleagues have reported that MGAT1 activity is higher for long-chain highly unsaturated MAGs, specifically MAG(20:4) (1). Whether these MAG species can directly inhibit adipocyte differentiation remains to be explored. We acknowledge these studies are limited as our lipidomics data represent static lipid abundance and not flux into glycerolipid synthesis. Thus, these differences may be indicative of impaired differentiation and not MGAT1 enzymatic function *per se*.

CONCLUSION

Here we have provided evidence that *Mogat1* expression initiates adipocyte differentiation in mouse iWAT preadipocytes. Furthermore, acute *Mogat1* knockout reduces adipogenic gene expression and glycerolipid accumulation in differentiated cells. HFD-fed adipocyte-specific *Mogat1* knockout mice have no discernable metabolic phenotype compared to littermate controls. These data suggest that there are compensatory mechanisms for loss of *Mogat1* and/or that adipocyte *Mogat1* expression is dispensable for diet-induced obesity in mice.

Supplementary Material

Refer to Web version on PubMed Central for supplementary material.

ACKNOWLEDGMENTS

We thank the Metabolomics Facility at Washington University (P30 DK020579) and the following investigators for their plasmid contributions to Addgene that were used in this research: Didier Trono, Bob Weinberg, Inder Verma, and Tyler Jacks. This publication is solely the responsibility of the authors and does not necessarily represent the official view of NCRR or NIH.

Funding:

This work was supported by grants from the NIH R56 DK111735 and the American Diabetes Association 1–17-IBS-109 to BNF, NIH K01 DK126990 to AJL, and core laboratories of Washington University School of Medicine: Digestive Diseases Research Cores Center NIH P30DK052574, Nutrition Obesity Research Center P30 DK056341 and the Diabetes Research Center NIH P30 DK020579.

REFERENCES

1. Yen C-LE, Farese RV. MGAT2, a Monoacylglycerol Acyltransferase Expressed in the Small Intestine. J Biol Chem 2003;278:18532–18537. [PubMed: 12621063]
2. Banh T, Nelson DW, Gao Y, Huang T-N, Yen M-I, Yen C-LE. Adult-onset deficiency of acyl CoA:monoacylglycerol acyltransferase 2 protects mice from diet-induced obesity and glucose intolerance. J Lipid Res 2015;56:379–389. [PubMed: 25535286]
3. Gao Y, Nelson DW, Banh T, Yen M-I, Yen C-LE. Intestine-specific expression of MOGAT2 partially restores metabolic efficiency in Mogat2-deficient mice. J Lipid Res 2013:jlr.M035493.
4. Liss KHH, Lutkewitte AJ, Pietka T, et al. Metabolic importance of adipose tissue monoacylglycerol acyltransferase 1 in mice and humans. J Lipid Res 2018:jlr.M084947.
5. Hall AM, Kou K, Chen Z, et al. Evidence for regulated monoacylglycerol acyltransferase expression and activity in human liver. J Lipid Res 2012;53:990–999. [PubMed: 22394502]
6. Yen C-LE, Stone SJ, Cases S, Zhou P, Farese RV. Identification of a gene encoding MGAT1, a monoacylglycerol acyltransferase. Proc Natl Acad Sci USA 2002;99:8512–8517. [PubMed: 12077311]
7. Lutkewitte AJ, Singer JM, Shew TM, et al. Multiple antisense oligonucleotides targeted against monoacylglycerol acyltransferase 1 (Mogat1) improve glucose metabolism independently of Mogat1. Mol Metab 2021;49.
8. Agarwal AK, Tunison K, Dalal JS, et al. Mogat1 deletion does not ameliorate hepatic steatosis in lipodystrophic (Agpat2−/−) or obese (ob/ob) mice. J Lipid Res 2016;57:616–630. [PubMed: 26880786]
9. Soufi N, Hall AM, Chen Z, et al. Inhibiting Monoacylglycerol Acyltransferase 1 Ameliorates Hepatic Metabolic Abnormalities but Not Inflammation and Injury in Mice. J Biol Chem 2014;289:30177–30188. [PubMed: 25213859]
10. Hall AM, Soufi N, Chambers KT, et al. Abrogating Monoacylglycerol Acyltransferase Activity in Liver Improves Glucose Tolerance and Hepatic Insulin Signaling in Obese Mice. Diabetes 2014;63:2284–2296. [PubMed: 24595352]
11. Porter LC, Franczyk MP, Pietka T, et al. NAD+-dependent deacetylase SIRT3 in adipocytes is dispensable for maintaining normal adipose tissue mitochondrial function and whole body metabolism. Am J Physiol Endocrinol Metab 2018;315:E520–E530. [PubMed: 29634313]
12. Craft CS, Pietka TA, Schappe T, et al. The extracellular matrix protein MAGP1 supports thermogenesis and protects against obesity and diabetes through regulation of TGF-β. Diabetes 2014;63:1920–1932. [PubMed: 24458361]
13. Lodhi IJ, Dean JM, He A, et al. PexRAP Inhibits PRDM16-Mediated Thermogenic Gene Expression. Cell Reports 2017;20:2766–2774. [PubMed: 28930673]
14. Hahn WC, Dessain SK, Brooks MW, et al. Enumeration of the Simian Virus 40 Early Region Elements Necessary for Human Cell Transformation. Molecular and Cellular Biology 2002.
15. Naviaux RK, Costanzi E, Haas M, Verma IM. The pCL vector system: rapid production of helper-free, high-titer, recombinant retroviruses. J Virol 1996;70:5701–5705. [PubMed: 8764092]

16. Kumar MS, Pester RE, Chen CY, et al. Dicer1 functions as a haploinsufficient tumor suppressor. Genes Dev 2009;23:2700–2704. [PubMed: 19903759]
17. Bligh EG, Dyer WJ. A rapid method of total lipid extraction and purification. Can J Biochem Physiol 1959;37:911–917. [PubMed: 13671378]
18. Sembongi H, Miranda M, Han G-S, et al. Distinct Roles of the Phosphatidate Phosphatases Lipin 1 and 2 during Adipogenesis and Lipid Droplet Biogenesis in 3T3-L1 Cells. J Biol Chem 2013;288:34502–34513. [PubMed: 24133206]
19. Chon S-H, Zhou YX, Dixon JL, Storch J. Intestinal monoacylglycerol metabolism: developmental and nutritional regulation of monoacylglycerol lipase and monoacylglycerol acyltransferase. J Biol Chem 2007;282:33346–33357. [PubMed: 17848545]
20. Qi J, Lang W, Connelly MA, et al. Metabolic tracing of monoacylglycerol acyltransferase-2 activity in vitro and in vivo. Analytical Biochemistry 2017;524:68–75. [PubMed: 27665677]
21. Cao J, Lockwood J, Burn P, Shi Y. Cloning and Functional Characterization of a Mouse Intestinal Acyl-CoA:Monoacylglycerol Acyltransferase, MGAT2. J Biol Chem 2003;278:13860–13866. [PubMed: 12576479]
22. Cao J, Burn P, Shi Y. Properties of the mouse intestinal acyl-CoA:monoacylglycerol acyltransferase, MGAT2. J Biol Chem 2003;278:25657–25663. [PubMed: 12730219]
23. Liss KHH, Ek SE, Lutkewitte AJ, et al. Monoacylglycerol acyltransferase 1 knockdown exacerbates hepatic ischemia-reperfusion injury in mice with hepatic steatosis. Liver Transplantation n/a.
24. Lutkewitte AJ, McCommis KS, Schweitzer GG, et al. Hepatic Monoacylglycerol Acyltransferase 1 is Induced by Prolonged Food Deprivation to Modulate the Hepatic Fasting Response. J Lipid Res 2019:jlr.M089722.
25. Hayashi Y, Suemitsu E, Kajimoto K, et al. Hepatic Monoacylglycerol O-acyltransferase 1 as a Promising Therapeutic Target for Steatosis, Obesity, and Type 2 Diabetes. Molecular Therapy - Nucleic Acids 2014;3.
26. Harris CA, Haas JT, Streeper RS, et al. DGAT enzymes are required for triacylglycerol synthesis and lipid droplets in adipocytes. J Lipid Res 2011;52:657–667. [PubMed: 21317108]
27. Chitraju C, Walther TC, Farese RV. The triglyceride synthesis enzymes DGAT1 and DGAT2 have distinct and overlapping functions in adipocytes. J Lipid Res 2019;60:1112–1120. [PubMed: 30936184]
28. Chitraju C, Mejhert N, Haas JT, et al. Triglyceride Synthesis by DGAT1 Protects Adipocytes from Lipid-Induced ER Stress during Lipolysis. Cell Metab 2017;26:407–418.e3. [PubMed: 28768178]
29. Phan J, Reue K. Lipin, a lipodystrophy and obesity gene. Cell Metabolism 2005;1:73–83. [PubMed: 16054046]
30. Csaki LS, Dwyer JR, Li X, et al. Lipin-1 and lipin-3 together determine adiposity in vivo. Molecular Metabolism 2014;3:145–154. [PubMed: 24634820]
31. Mitra MS, Chen Z, Ren H, et al. Mice with an adipocyte-specific lipin 1 separation-of-function allele reveal unexpected roles for phosphatidic acid in metabolic regulation. PNAS 2013;110:642–647. [PubMed: 23267081]
32. Nadra K, Médard J-J, Mul JD, et al. Cell Autonomous Lipin 1 Function Is Essential for Development and Maintenance of White and Brown Adipose Tissue. Molecular and Cellular Biology 2012;32:4794–4810. [PubMed: 23028044]
33. Phan J, Péterfy M, Reue K. Lipin Expression Preceding Peroxisome Proliferator-activated Receptor-γ Is Critical for Adipogenesis in Vivo and in Vitro. J Biol Chem 2004;279:29558–29564. [PubMed: 15123608]
34. Koh Y-K, Lee M-Y, Kim J-W, et al. Lipin1 Is a Key Factor for the Maturation and Maintenance of Adipocytes in the Regulatory Network with CCAAT/Enhancer-binding Protein α and Peroxisome Proliferator-activated Receptor γ2. J Biol Chem 2008;283:34896–34906. [PubMed: 18930917]
35. Péterfy M, Phan J, Xu P, Reue K. Lipodystrophy in the fld mouse results from mutation of a new gene encoding a nuclear protein, lipin. Nature Genetics 2001;27:121. [PubMed: 11138012]
36. Petersen RK,JØrgensen C, Rustan AC, et al. Arachidonic acid-dependent inhibition of adipocyte differentiation requires PKA activity and is associated with sustained expression of cyclooxygenases. Journal of Lipid Research 2003;44:2320–2330. [PubMed: 12923227]

37. Haugen F, Zahid N, Dalen KT, Hollung K, Nebb HI, Drevon CA. Resistin expression in 3T3-L1 adipocytes is reduced by arachidonic acid. J Lipid Res 2005;46:143–153. [PubMed: 15489540]

38. Kim H-K, Della-Fera M, Lin J, Baile CA. Docosahexaenoic Acid Inhibits Adipocyte Differentiation and Induces Apoptosis in 3T3-L1 Preadipocytes. J Nutr 2006;136:2965–2969. [PubMed: 17116704]

STUDY IMPORTANCE

What is already known?

- Adipose tissue expansion through adipocyte precursor cell differentiation is critical for proper lipid storage during nutrient overload.
- Monoacylglycerol O-acyltransferase 1 (*Mogat1*), a lipogenic enzyme, is highly induced during adipocyte differentiation of human and mouse precursor cells and is reduced in patients with obesity and metabolic dysfunction.

What does this study add?

- *Mogat1* deletion during early adipocyte differentiation reduces differentiation capacity, and adipogenic gene expression and lowers glycerolipid content of differentiated adipocytes.
- Adipocyte *Mogat1* expression is dispensable for adiposity and metabolic outcomes in high-fat-fed mice and suggests compensation from other glycerolipid synthesis enzymes.

How might these results change the direction of research?

- These results provide a better understanding of the molecular mechanisms of glycerolipid metabolism and healthy adipose tissue expansion.

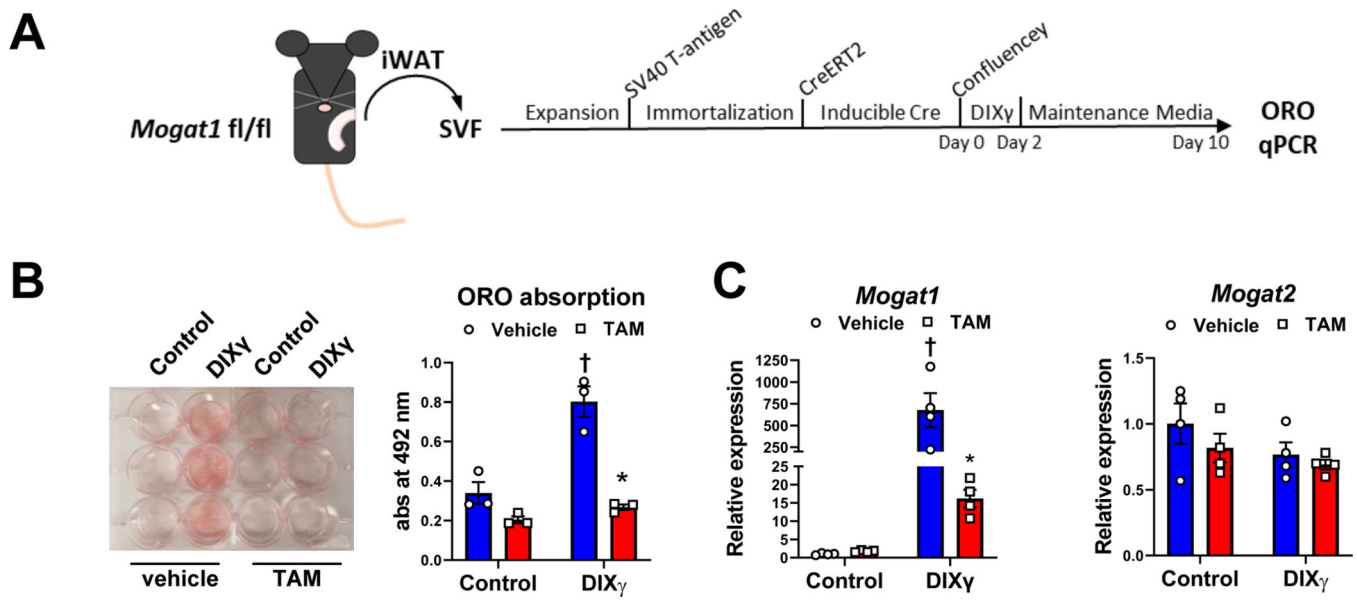

Figure 1: *Mogat1* expression is required for adipocyte differentiation initiation *in vitro*.

Stromal vascular fractions (SVF) were isolated from iWAT adipose tissue of *Mogat1* fl/fl mice. Cells were immortalized with SV40 T antigen prior to transfection with an inducible CreERT2. **A:** Diagram of the treatment protocol for the generation of SVF and inducible *Mogat1* cell lines as described in the methods **B, C:** Cre recombinase activity to delete *Mogat1* was activated with the addition of 4 nM tamoxifen on Day 0 while other cells were treated with vehicle. **B:** After 10 days of differentiation, lipid accumulation was reduced by *Mogat1* knockout as shown by a representative ORO staining and quantification by extraction and measuring absorption at 492nm. **C:** Gene expression analysis as measured by qPCR. *Mogat1* gene expression is induced by differentiation and inhibited by TAM while *Mogat2* was unaffected by differentiation or TAM treatment. Data are expressed as mean ± S.E.M. Two-way ANOVA was performed followed by Tukey's multiple comparisons tests, * $p < 0.05$ vs. vehicle, † $p < 0.05$ vs. control undifferentiated cells; $n = 3–4$ biological replicates.

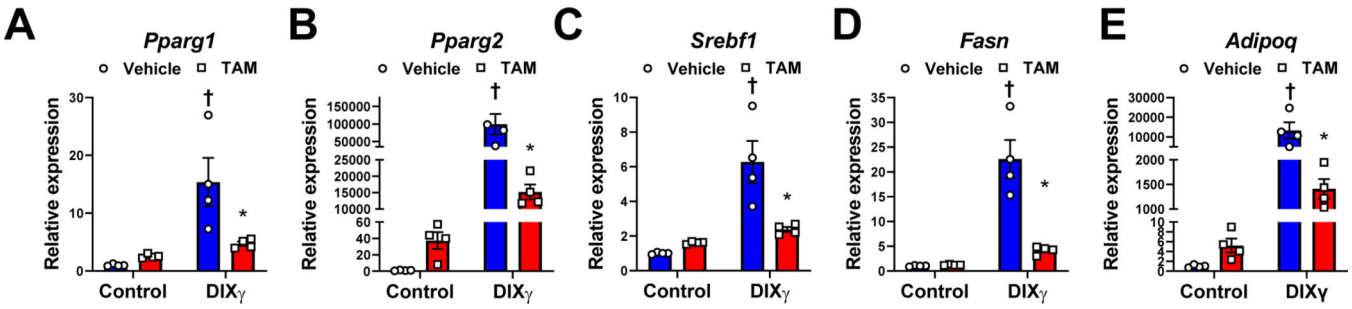

Figure 2: *Mogat1* is required for adipogenic gene expression *in vitro*.

Confluent cells were treated with tamoxifen (4 nM) at the onset of differentiation (via DIXγ cocktail) and harvested after 10 days. **A-E:** Gene expression analysis as measured by qPCR: *Peroxisome proliferator-activated receptor gamma (Pparg) 1* and *2, Sterol regulatory element-binding transcription factor 1 (Srebf1), Fatty acid synthase (Fasn),* and *Adiponectin (Adipoq)* were increased during differentiation and reduced by *Mogat1* knockout. Data are expressed as mean ± S.E.M. Two-way ANOVA was performed followed by Tukey's multiple comparisons tests, * $p < 0.05$ vs. vehicle, † $p < 0.05$ vs. control undifferentiated cells; $n = 4$ biological replicates.

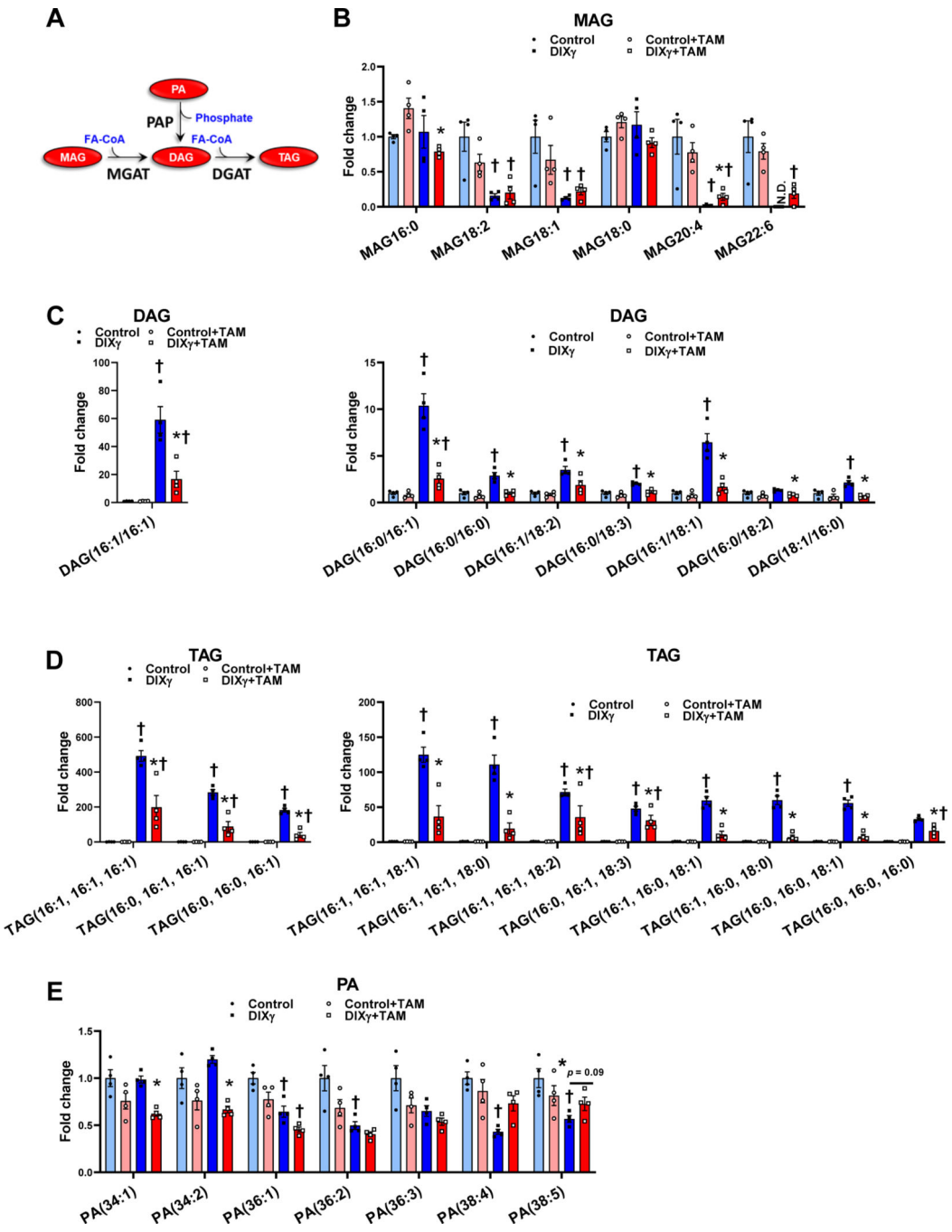

Figure 3: *Mogat1* knockout prevents the accumulation of glycerolipids in differentiated SVF cells.

Confluent cells were treated with tamoxifen (4 nM) at the onset of differentiation (via DIXγ cocktail) and harvested after 10 days. **A:** Depiction of lipids analyzed via LC-MS/MS **B-E:** Lipid content was lowered by *Mogat1* knockout. Data are expressed as mean ± S.E.M. Two-way ANOVA was performed followed by Tukey's multiple comparisons tests, * $p < 0.05$ vs. vehicle, † $p < 0.05$ vs. control undifferentiated cells; $n = 4$ biological replicates.

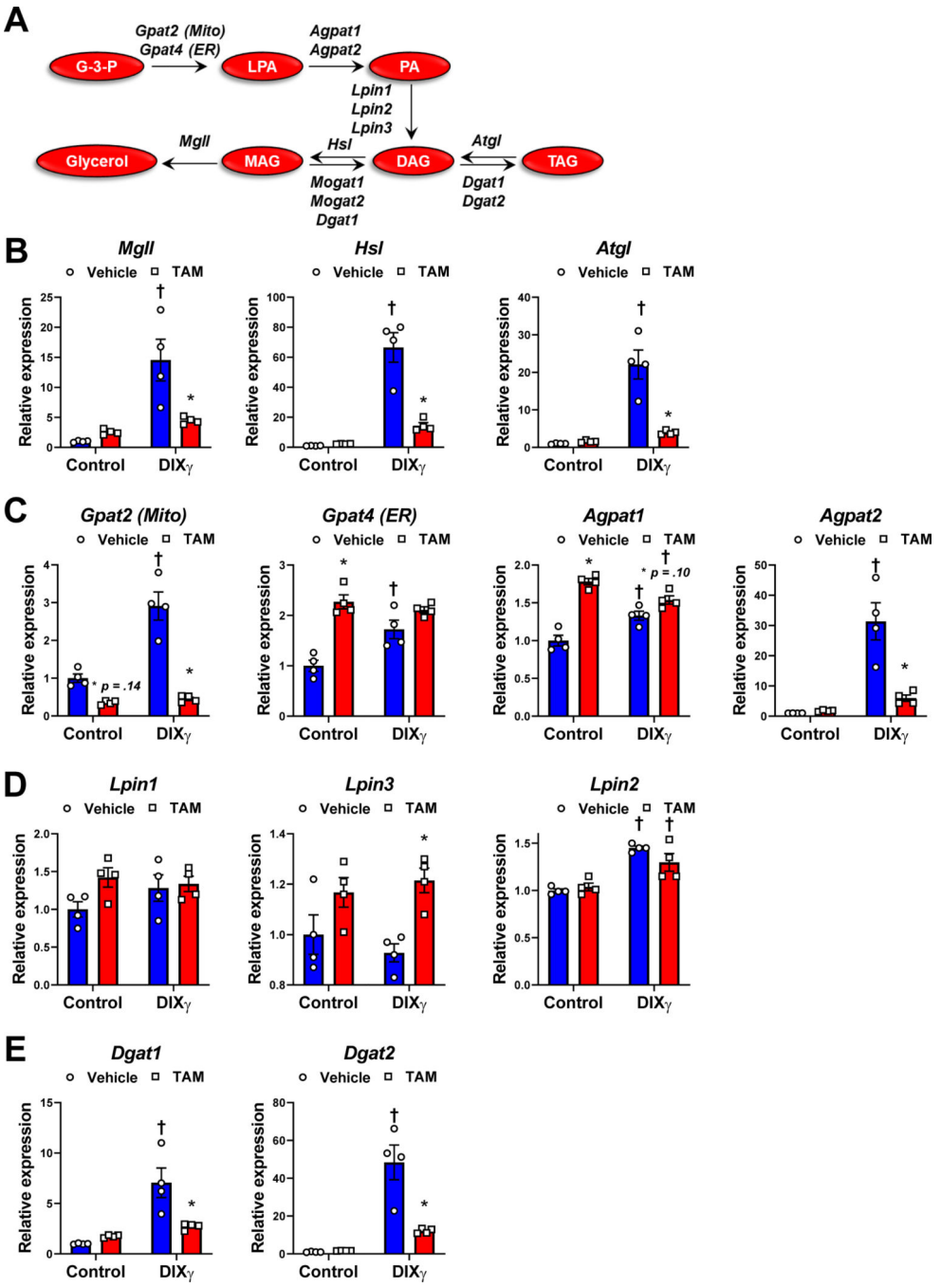

Figure 4: Deletion of *Mogat1* attenuates the induction of triglyceride synthetic enzymes during adipogenesis *in vitro*.

Confluent cells were treated with tamoxifen (4 nM) at the onset of differentiation (via DIXγ cocktail) and harvested after 10 days. **A-D:** Gene expression analysis as measured by qPCR**. A:** Depiction of gene networks analyzed **B:** Lipolytic genes *Monoacylglycerol lipase (Mgll), Hormone sensitive lipase (Hsl), Adipose triglyceride lipase (Atgl)* **C:** Glycerol-3-phoshate pathway intermediates genes *glycerol-3-phosphate acyltransferase* (*Gpat2, mitochondrial (Mito) isoform & 4 endoplasmic reticulum (ER*) isoform) and *1-acylglycerol-3-phosphate*

O-acyltransferase (*Agpat1 & 2)* **D:** *Phosphatidate phosphohydrolases (Lpin1,2, & 3)*. **E:** *Diacylglycerol O-acyltransferase 1 and 2 (Dgat1 & 2)*. Data are expressed as mean ± S.E.M. Two-way ANOVA was performed followed by Tukey's multiple comparisons tests, * $p < 0.05$ vs. vehicle, † $p < 0.05$ vs. control undifferentiated cells; $n = 4$ biological replicates.

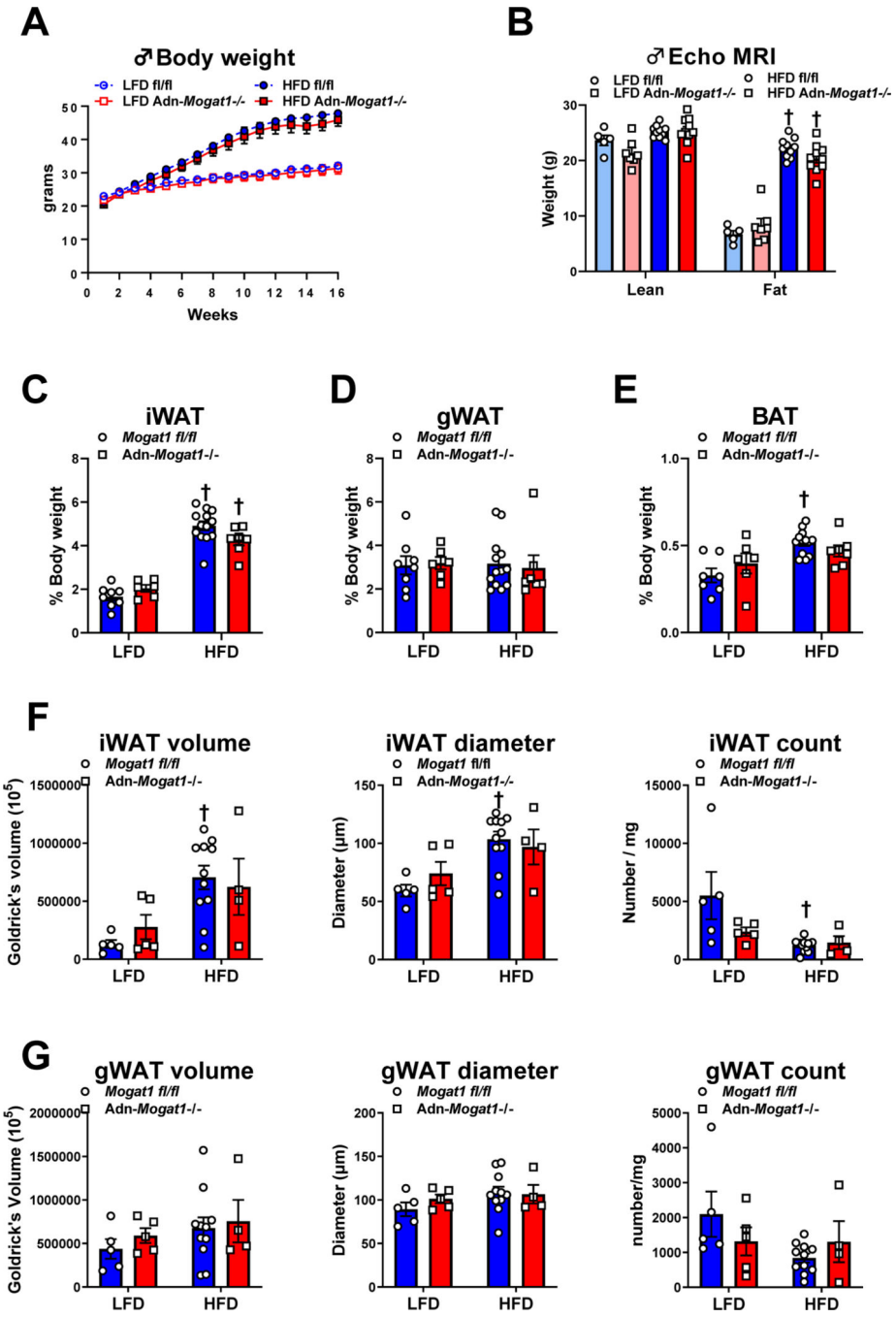

Figure 5. Adipocyte-Specific *Mogat1* knockout mice gain similar weight on a long-term high-fat diet compared to littermate controls.

Male adipocyte-specific *Mogat1* fl/fl knockout mice (Adn-*Mogat1*−/−) and littermate controls (*Mogat1* fl/fl) were fed a 10% (kcal % fat) low-fat diet (LFD) or a 60% (kcal % fat) high-fat diet (HFD) starting at eight weeks of age. After 16 weeks of diet, mice were fasted for 4 hours prior to sacrifice and tissue collection. **A:** HFD-fed mice gained more weight compared to LFD-fed controls and was unaffected by genotype. **B:** After 15 weeks of diet, HFD-fed mice had increased fat mass compared to LFD-fed mice as measured by

ECHO MRI. **C-E:** inguinal white adipose tissue (iWAT) and gonadal white adipose tissue (gWAT) but not brown adipose tissue (BAT) were increased by HFD and are expressed as % total body weight. **F, G:** Samples from iWAT and gWAT were fixed and dissociated. Liberated adipocytes were measured and counted. Data are expressed as mean ± S.E.M. Two-way ANOVA was performed followed by Tukey's multiple comparisons tests, † $p < 0.05$ vs. LFD; $n = 5–12$ in **A-E** and 4–11 in **F, G**.

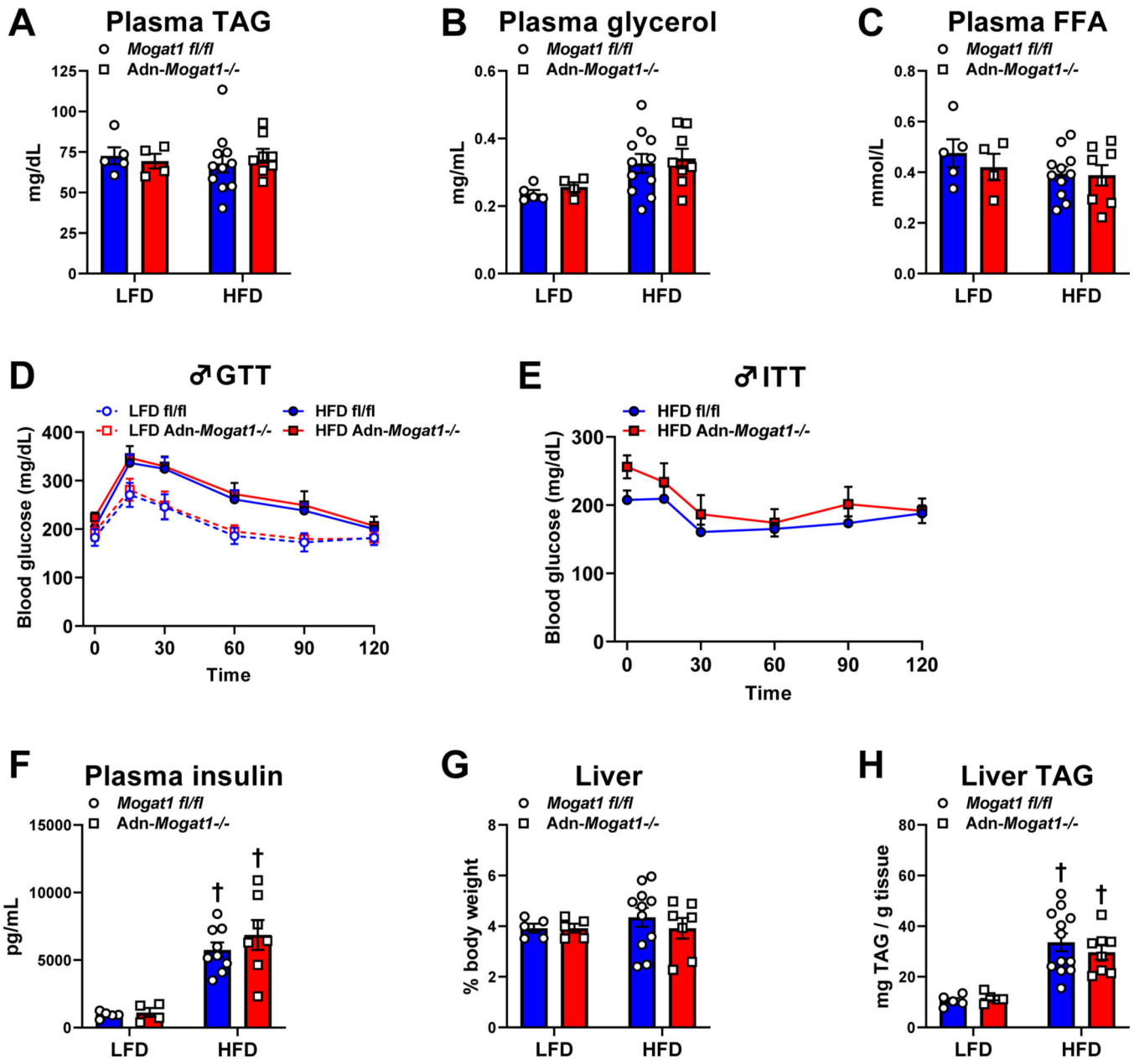

Figure 6. Adn-*Mogat1*−/− mice have a similar metabolic profile as littermate controls.

Male Adn-*Mogat1*−/− and littermate control mice were fed a 10% LFD or a 60% HFD starting at eight weeks of age. After 16 weeks of diet, mice were fasted for 4 hours prior to sacrifice and tissue collection. **A-C:** Plasma triglycerides (TAG), glycerol, and free fatty acids (FFA) were measured enzymatically using commercially available colorimetric assays. **D, E:** Glucose tolerance tests (GTT, 1 g/Kg lean mass, 5 hour fast) and insulin tolerance tests (ITT, 0.75 U/Kg lean mass, 4 hour fast) were measured at 16 weeks and 15 weeks and were similar between groups. **F:** Four-hour fasted plasma insulin levels measured at sacrifice were increased by HFD feeding. **G:** Liver weight as a % total body weight was not changed by diet or genotype. **H:** Liver triglycerides (TAG) were measured as described above and were increased by HFD feeding. Data are expressed as mean ± S.E.M. Two-way ANOVA

was performed followed by Tukey's multiple comparisons tests, † $p < 0.05$ vs. LFD; $n =$ 4–12.

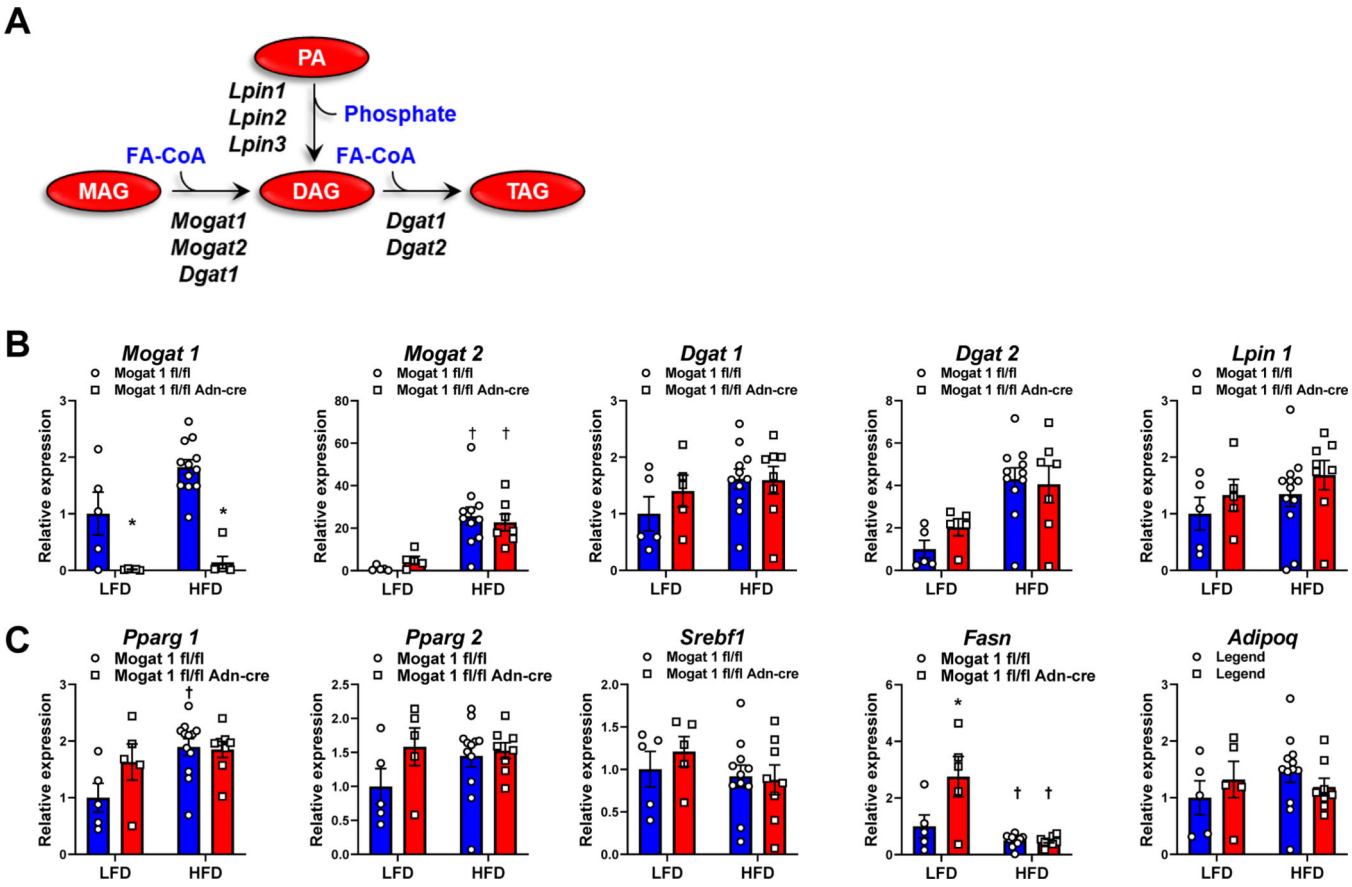

Figure 7. Subcutaneous adipose tissue from adipocyte-specific *Mogat1* knockout mice have a similar gene expression profile as littermate controls.

Male Mogat1 fl/fl and littermate adiponectin Cre+ (Adn-*Mogat1*−/−) mice were fed a 10% low-fat diet (LFD) or a 60% (HFD) starting at eight weeks of age. After 16 weeks of diet, mice were fasted for 4 hours prior to sacrifice and tissue collection. A schematic of genes involved in TAG metabolism. B, C: Subcutaneous iWAT adipose tissue gene expression analysis as measured by qPCR. A: *Mogat1, Mogat2, Dgat1* and *2,* and *Lpin1*. B: *Peroxisome proliferator-activated receptor gamma (Pparg) 1* and *2, Sterol regulatory element-binding transcription factor 1 (Srebf1), Fatty acid synthase (Fasn),* and *Adiponectin (Adipoq)* Data are expressed as mean ± S.E.M. Two-way ANOVA was performed followed by Tukey's multiple comparisons tests, * $p < 0.05$ vs. *fl/fl*, † $p < 0.05$ vs. LFD; $n = 5–11$.